Finding a nonlinear lattice with improved integrability using Lie transform perturbation theory

Kiran G. Sonnad and John. R. Cary
Center for Integrated Plasma Studies and Department of Physics, University of Colorado, Boulder, Colorado 80309, USA
(Received 12 October 2003; published 12 May 2004)

A condition for improved dynamic aperture for nonlinear, alternating gradient transport systems is derived using Lie transform perturbation theory. The Lie transform perturbation method is used here to perform averaging over fast oscillations by canonically transforming to slowly oscillating variables. This is first demonstrated for a linear sinusoidal focusing system. This method is then employed to average the dynamics over a lattice period for a nonlinear focusing system, provided by the use of higher order poles such as sextupoles and octupoles along with alternate gradient quadrupoles. Unlike the traditional approach, the higher order focusing is not treated as a perturbation. The Lie transform method is particularly advantageous for such a system where the form of the Hamiltonian is complex. This is because the method exploits the property of canonical invariance of Poisson brackets so that the change of variables is accomplished by just replacing the old ones with the new. The analysis shows the existence of a condition in which the system is azimuthally symmetric in the transformed, slowly oscillating frame. Such a symmetry in the time averaged frame renders the system nearly integrable in the laboratory frame. This condition leads to reduced chaos and improved confinement when compared to a system that is not close to integrability. Numerical calculations of single-particle trajectories and phase space projections of the dynamic aperture performed for a lattice with quadrupoles and sextupoles confirm that this is indeed the case.

DOI: 10.1103/PhysRevE.69.056501 PACS number(s): 29.27.−a, 45.10.Hj, 05.45.Gg

I. INTRODUCTION

Linear focusing systems such as the alternate gradient quadrupole systems are relatively easy to analyze because of the existence of the Courant-Snyder invariants [1], which reduce the system to an uncoupled set of systems of one degree of freedom. In the presence of higher order components such as sextupoles or octupoles, these invariants are destroyed. Such a system is nonintegrable and has trajectories that are chaotic and poorly confined. Despite this shortcoming in the use of nonlinear components, their use has been proposed in a variety of applications. They include, for example, achieving uniform particle distributions [2], control of beam emittance growth and beam halo formation [3,4], providing strong sextupole focusing in planar undulators in free electron lasers [3], folding of beam phase space distributions as an alternate to beam collimation [4], introducing Landau damping by providing octupole or sextupole induced tune spread [5,6], photoelectron trapping in quadrupole and sextupole magnetic fields [7], etc. In addition to this sextupoles are widely used in storage rings for cromaticity corrections. Nonlinear forces also arise as a result of beam-beam interactions at interaction point of a storage ring collider which limit the dynamic aperture of the system [8]. Thus, a general analysis of the nonlinear focusing problem is important. It is well known that a near integrable Hamiltonian system will typically possess regular trajectories intermingled with regions of chaos. The aim of this paper is to find a condition that optimizes the integrability of the system thereby minimizing the chaotic region in the presence of certain nonlinear focusing components.

To perform the analysis we use the Lie transform perturbation method, which exploits the invariance of the Poisson brackets under canonical transformations. In this analysis all dynamical variables appear within Poisson brackets, so the whole formulation is canonically invariant. If this were not true, one would need to express the Hamiltonian in terms of the new variables up to the desired order before performing the perturbation analysis. This could make the problem more tedious when the form of the Hamiltonian is not simple, and when it is required to carry the expansion up to third order, both of which are true in this case. References [9–11] contain other procedures for averaging applied to beam physics. We follow the Lie transform method described in Ref. [12] and show that rearranging the different order terms of the Hamiltonian in this method enables one to perform a time averaging rather than average the motion over the trajectory described by the integrable component of the Hamiltonian.

To start with, Sec. II provides a brief description of the Lie transform method used in this paper. Section III presents an illustration of the method applied to a continuous periodic focusing system, an example also used by Channel [9]. In Sec. IV, we introduce a nonlinear focusing system which has a higher order multipoles in addition to quadrupoles. The resulting Hamiltonian describing the motion transverse to the beam propagation is nonautonomous and has two degrees of freedom. By averaging the motion over the lattice period up to third order, we derive a condition for the new time-independent Hamiltonian to also be independent of the transformed azimuthal variable. Under such a condition, the transformed angular momentum will be an adiabatic invariant. It will be shown that this condition is satisfied when the functions describing the forces due to the respective multipole are orthogonal to each other in a certain manner.

In order to show that the condition of azimuthal invariance is a desirable one, various numerical calculations are performed. Section V includes results which show that as one deviates from the desired condition, the particle oscillations acquire additional frequency components and also have larger oscillation amplitudes. Section VI illustrates the pro-

jection of the dynamic aperture on to different planes in phase space. The dynamic aperture is the region that allows what may be defined as confined particles. Estimating the dynamic aperture for different cases shows that maximum confinement can be achieved when the associated time averaged Hamiltonian is integrable in the transformed coordinates and hence the system is nearly integrable in the laboratory frame. The dynamic aperture is shown to gradually diminish in size as one deviates from this condition.

II. THE LIE TRANSFORM METHOD FOR AVERAGING OVER FAST OSCILLATIONS

In this section we outline the Hamilton perturbation method described in Ref. [12]. This method is based on previous work [13–17] that introduced Lie transform theory as a convenient method to perform Hamilton perturbation analysis. The Lie transformation is defined with respect to a phase space function w such that it satisfies the following Poisson bracket relationship:

$$\frac{d\mathbf{Z}}{d\epsilon} = \{\mathbf{Z}, w(\mathbf{Z}(\mathbf{z},t,\epsilon),t,\epsilon)\}, \tag{1}$$

where $\mathbf{Z}=(\mathbf{P},\mathbf{Q})$ is a phase space vector representing the generalized positions and momenta of the system, w is the Lie generating function, and ϵ is a continuously varying parameter such that $\mathbf{Z}(\epsilon=0)=\mathbf{z}$, the original phase space vector. The above relationship resembles Hamilton's equation with respect to a "Hamiltonian," w and "time," ϵ. This guarantees that the transformation is canonical for all values of ϵ.

The Lie operator L is defined such that it performs a Poisson bracket operation with respect to w. Symbolically,

$$L = \{w,\}. \tag{2}$$

A transformation operator T is defined such that its role is to replace the variables of a function by the new canonical variables. For the identity function this is simply,

$$T\mathbf{z} = \mathbf{Z}(\mathbf{z},\epsilon,t). \tag{3}$$

The operator T is analogous to the "evolution" operator with respect to ϵ. Using Eq. (1) it can be verified that T satisfies

$$\frac{dT}{d\epsilon} = -TL. \tag{4}$$

For a similar relationship involving the inverse transformation operator T^{-1}, we differentiate the equation $TT^{-1}=1$ and use the above equation to obtain

$$\frac{dT^{-1}}{d\epsilon} = T^{-1}L. \tag{5}$$

The transformed Hamiltonian K can be expressed in terms of the original Hamiltonian $\mathcal{H}$ as

$$K(\epsilon) = T^{-1}(\epsilon)(\mathcal{H}) + T^{-1}(\epsilon)\int_0^\epsilon d\epsilon' T(\epsilon')\frac{\partial w}{\partial t}(\epsilon'). \tag{6}$$

This expression was obtained by Dewar [16].

To obtain explicit equations for each perturbation term, every physical quantity and operator is expressed as a power series in ϵ known as the Deprit power series [15]. The original and transformed Hamiltonians are given by $H(\mathbf{z},\epsilon,t)=\sum_{n=0}^{\infty}\epsilon^n H_n(\mathbf{z},t)$, $K(\mathbf{z},\epsilon,t)=\sum_{n=0}^{\infty}\epsilon^n K_n(\mathbf{z},t)$. The Lie generating function is represented a little differently because it appears as a derivative in Eq. (6). This is, $w(\mathbf{z},t,\epsilon)=\sum_{n=0}^{\infty}\epsilon^n w_{n+1}(\mathbf{z},t)$. The operators T and L are represented in a similar way as $T(t,\epsilon)=\sum_{n=0}^{\infty}\epsilon^n T_n(t)$, $L(w)=\sum_{n=0}^{\infty}\epsilon^n L_n$, where $L_n=\{w_n,\}$, the Poisson bracket with respect to w_n. The parameter ϵ is used to keep track of the terms representing different orders in the expansion and is usually set to one in the end.

By substituting the Deprit expansions into Eqs. (4), (5), and (6), one can obtain relationships between the corresponding terms for each order of ϵ. Doing this for Eq. (6), we get, up to third order,

$$K_0 = H_0, \tag{7a}$$

$$\frac{\partial w_1}{\partial t} + \{w_1,H_0\} = K_1 - H_1, \tag{7b}$$

$$\frac{\partial w_2}{\partial t} + \{w_2,H_0\} = 2(K_2 - H_2) - L_1(K_1 + H_1), \tag{7c}$$

$$\frac{\partial w_3}{\partial t} + \{w_3,H_0\} = 3(K_3 - H_3) - L_1(K_2 + 2H_2) - L_2\left(K_1 + \frac{1}{2}H_1\right) - \frac{1}{2}L_1^2 H_1. \tag{7d}$$

The expression $\partial w_n/\partial t + \{w_n,H_0\}$ is the variation of w_n along the unperturbed trajectory described by H_0. Setting $H_0=0$ reduces this to a partial derivative with respect to t. Thus, instead of integrating along the unperturbed trajectory, we simply perform an integration over time to determine w_n. At each order, K_n is chosen such that it cancels the terms that average to a nonzero value over fast oscillations. As a result, the corresponding value of w_n will have a zero average. This is necessary to prevent w_n from being secular (unbounded) in time [12].

Using Eq. (5), and the Deprit series expression for the operators L and T, the inverse transformation operator to third order may be expressed as

$$T_0^{-1} = I, \tag{8a}$$

$$T_1^{-1} = L_1, \tag{8b}$$

$$T_2^{-1} = \tfrac{1}{2}L_2 + \tfrac{1}{2}L_1^2, \tag{8c}$$

$$T_3^{-1} = \tfrac{1}{3}L_3 + \tfrac{1}{6}L_1L_2 + \tfrac{1}{3}L_2L_1 + \tfrac{1}{6}L_1^3. \tag{8d}$$

It may be noted that when L, T, and T^{-1} act upon any phase space function, they are expressed in the form of Poisson brackets, which are independent of the canonical variables used. This makes the whole formulation canonically invariant. For a systematic derivation of all these relation-

ships one may refer to Ref. [12] where they are given up to fourth order. A shorter description of the same may be found in Ref. [18].

III. APPLICATION TO A LINEAR SINUSOIDAL FOCUSING SYSTEM

As an illustration and a test for the validity of the method, we perform the analysis for a linear periodic focusing system. The same example was used in Ref. [9] for the method developed in that paper. The single-particle Hamiltonian associated with such a system is given by

$$H = \frac{p^2}{2} + \frac{kq^2}{2}\sin(\omega t). \tag{9}$$

This Hamiltonian also describes the motion of a particle in systems such as the Paul trap and the ponderomotive potential. We apply Eqs. (7) to perform the averaging. As explained in the preceding section, we set $H_0=0$ and $H_1=H$. From Eq. (7a) we get

$$K_0 = H_0 = 0. \tag{10}$$

Applying the first-order relationship, Eq. (7b), we get

$$\frac{\partial w_1}{\partial t} = K_1 - \frac{p^2}{2} - \frac{kq^2}{2}\sin(\omega t). \tag{11}$$

The third term on the right averages to zero with respect to time. In order that the net result average to zero, we require

$$K_1 = \frac{p^2}{2}. \tag{12}$$

Since w_1 is relevant only up to an additive constant, it is sufficient to evaluate the indefinite integral to determine w_1, hence

$$w_1 = \frac{kq^2}{2\omega}\cos(\omega t). \tag{13}$$

The second-order equation, Eq. (7c), gives

$$\frac{\partial w_2}{\partial t} = 2K_2 - \frac{2kpq}{\omega}\cos(\omega t). \tag{14}$$

Since the second term on the right side averages to zero, we choose

$$K_2 = 0, \tag{15}$$

and so,

$$w_2 = -\frac{2kqp}{\omega^2}\sin(\omega t). \tag{16}$$

Applying the third-order relationship, Eq. (10) then gives

$$\frac{\partial w_3}{\partial t} = 3K_3 + \frac{3p^2k}{\omega^2}\sin(\omega t) - \frac{k^2q^2}{\omega^2}\sin^2(\omega t) - \frac{k^2q^2}{2\omega^2}\cos^2(\omega t). \tag{17}$$

Note that the third and fourth terms on the right side do not average to zero. In order that they cancel, we set

$$K_3 = \frac{1}{4}\frac{k^2q^2}{\omega^2} \tag{18}$$

and as a result,

$$w_3 = -\frac{3p^2k}{\omega^3}\cos(\omega t). \tag{19}$$

Collecting the nonzero terms, the transformed Hamiltonian is now given as a function of the new variables by

$$K = \frac{P^2}{2} + \frac{\Omega^2 Q^2}{2}, \tag{20}$$

where $\Omega = k/\sqrt{2}\omega$. This is the Hamiltonian for a harmonic oscillator with solution

$$Q(t) = Q(0)\cos(\Omega t) + \frac{P(0)}{\Omega}\sin(\Omega t), \tag{21}$$

$$P(t) = P(0)\cos(\Omega t) - \Omega Q(0)\sin(\Omega t). \tag{22}$$

To transform back to the original coordinate system, we use the operator T^{-1} for which we need to know L up to the desired order. The operators L_n can be expressed in terms of the values of w_n as

$$L_1 = \left\{ \frac{kQ^2}{2\omega}\cos(\omega t), \right\}, \tag{23}$$

$$L_2 = \left\{ -\frac{2kQP}{\omega^2}\sin(\omega t), \right\}, \tag{24}$$

$$L_3 = \left\{ -\frac{3kP^2}{\omega^3}\cos(\omega t), \right\}. \tag{25}$$

Using these to perform the inverse transformation as described by Eqs. (8), we get, up to third order,

$$q = Q + \frac{kQ}{\omega^2}\sin(\omega t) + \frac{2kP}{\omega^3}\cos(\omega t), \tag{26}$$

$$p = P + \frac{kQ}{\omega}\cos(\omega t) - \frac{kP}{\omega^2}\sin(\omega t) + \frac{1}{3}\frac{k^2}{\omega^3}Q\,\sin(\omega t)\cos(\omega t). \tag{27}$$

The above solution is compared with calculations from a fourth-order symplectic integrator [19,20] and is shown in Figs. 1 and 2. The parameters used were the same as those used in Ref. [9]. The accuracy of the approximate solution compares well with that obtained by Channel [9] using a different method. That is, the solution given by Eqs. (26) and (27) overlaps well with the numerical solution for $k/\omega^2 = 1/16$ and the accuracy gradually decreases with decreasing ω.

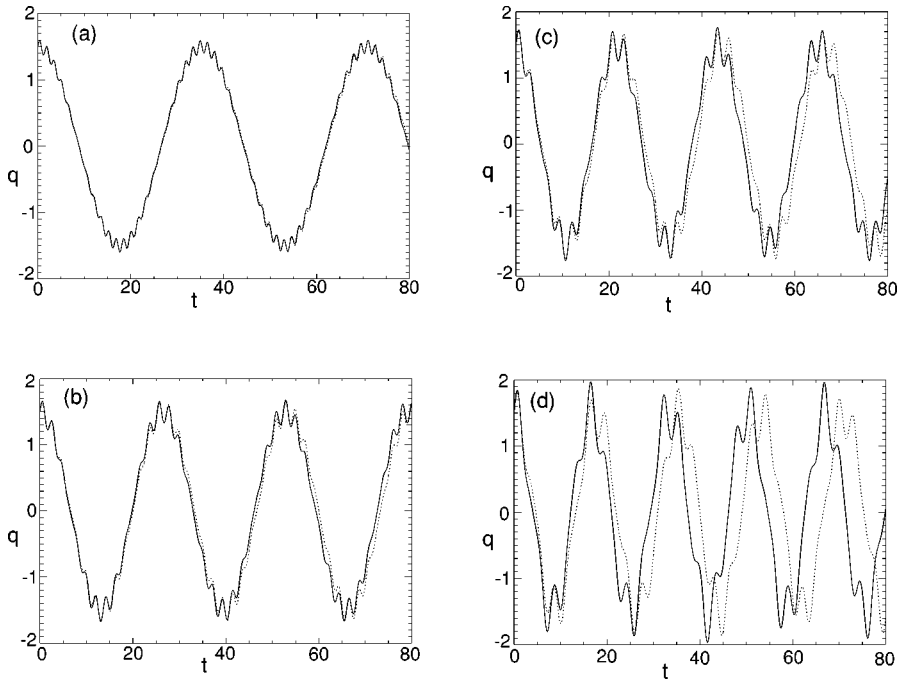

FIG. 1. q vs t with $k=1$, $\omega=$(a)4 , (b) 3, (c) 2.5, and (d) 2. The solid line represents the numerical solution.

IV. SINGLE PARTICLE AVERAGING FOR A NONLINEAR LATTICE

A. Alternate gradient sextupoles and quadrupoles

The external magnetic fields in the beam channel are expected to satisfy Maxwell's equations in vacuum which are given by $\vec{\nabla}\times\vec{B}=0$, $\vec{\nabla}\cdot\vec{B}=0$. The two-dimensional multipole expansion expression for such a magnetic field is

$$B_y + iB_x = B_0 \sum_{n=0}^{\infty} (b_n + ia_n)(x+iy)^n. \tag{28}$$

Ideally, b_n and a_n must be constants for the above to be valid. However, when analyzing alternate gradient focusing systems, they are regarded as step functions of the axial distance. This is still valid if fringe effects are disregarded.

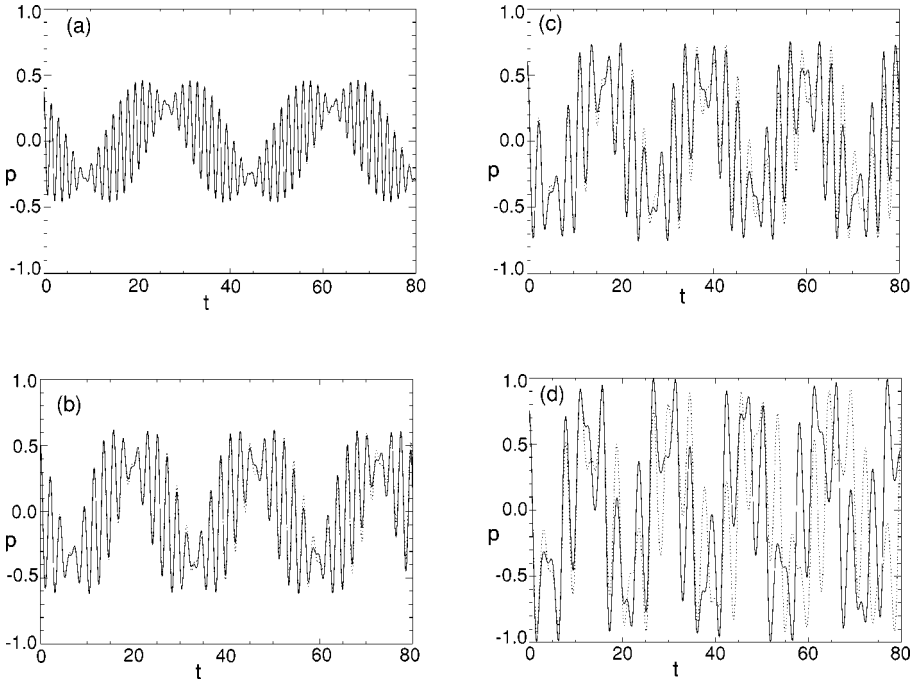

FIG. 2. p vs t with $k=1$, $\omega=$(a)4, (b) 3, (c) 2.5, and (d) 2. The solid line represents the numerical solution.

The orientation of the reference frame can be chosen such that $a_1=0$. Assuming the presence of only quadrupole ($n=1$) terms and sextupole ($n=2$) terms, b_1, a_2 and b_3 will generally be nonzero. The velocity of the particle in the z direction is assumed to be constant. The resulting Hamiltonian can be obtained from the Lorentz force. In cylindrical coordinates it is,

$$H=\frac{1}{2}\left(p_r^2+\frac{l^2}{r^2}\right)+\frac{1}{2}\kappa_2(s)r^2\cos(2\theta)+\frac{1}{3}\kappa_3(s)r^3\cos(3\theta+\alpha). \tag{29}$$

The variable s is the distance along the axis, which is equivalent to time for constant axial velocity. The momentum in the radial direction is p_r and l is the angular momentum. The values of $\kappa_2(s)$ and $\kappa_3(s)$ depend upon the strength of the quadrupole and sextupole magnets, respectively, and also the velocity of the particle in the axial direction. The angle α depends upon the relative values of a_2 and b_2, which is determined by the orientation of the sextupoles with respect to the quadrupoles. We use normalized units in which the charge and mass of the particle are unity. It is assumed that the Hamiltonian is periodic in s with periodicity S, i.e., $\kappa_2(s+S)=\kappa_2(s)$ and $\kappa_3(s+S)=\kappa_3(s)$. It is further assumed that the average of $\kappa_2(s)$ and $\kappa_3(s)$ over a period S is zero. That is,

$$\langle\kappa_2\rangle=\frac{1}{S}\int_s^{s+S}\kappa_2(s)ds=0 \tag{30}$$

and the same for κ_3. The angular brackets $\langle\cdots\rangle$ denote an average over one period in the rest of this section. With these conditions, κ_2 and κ_3 can in general be represented in the form of Fourier series as

$$\kappa_2(s)=\sum_{n=1}^{n=\infty}f_n\sin\left(\frac{2n\pi s}{S}\right)+\sum_{n=1}^{n=\infty}g_n\cos\left(\frac{2n\pi s}{S}\right) \tag{31}$$

and

$$\kappa_3(s)=\sum_{n=1}^{n=\infty}k_n\sin\left(\frac{2n\pi s}{S}\right)+\sum_{n=1}^{n=\infty}l_n\cos\left(\frac{2n\pi s}{S}\right). \tag{32}$$

However, the analysis in this section will show that it would be desirable for the above series to satisfy certain restrictions.

The averaging procedure to follow is valid when the averaged orbits are slowly varying over one lattice period S. The procedure is identical to the one used in the preceding section except that the algebra is more tedious since the Hamiltonian is more complex. Once again, we set $H_0=0$ and $H_1=H$. From Eq. (7b) we get $K_0=H_0=0$. Equation (7c) yields

$$\frac{\partial w_1}{\partial s}=K_1-\frac{1}{2}\left(p_r^2+\frac{l^2}{r^2}\right)-\frac{1}{2}\kappa_2(s)r^2\cos(2\theta)-\frac{1}{3}\kappa_3(s)r^3\cos(3\theta+\alpha). \tag{33}$$

From Eqs. (31) and (32) it follows that $\langle\kappa_2^{\mathrm{I}}\rangle=\langle\kappa_3^{\mathrm{I}}\rangle=0$. The roman numerical superscript indicates an integral over s with a constant of integration chosen so that the integral has a zero average over one lattice period S. Similarly, a superscript "II" will indicate a double integration over s with the same conditions, and so on. Choosing K_1 to cancel the terms with a nonzero average value then gives

$$K_1=\frac{1}{2}\left(p_r^2+\frac{l^2}{r^2}\right). \tag{34}$$

Integrating Eq. (39) yields

$$w_1=-\left[\tfrac{1}{2}\kappa_2^{\mathrm{I}}(s)r^2\cos(2\theta)+\tfrac{1}{3}\kappa_3^{\mathrm{I}}(s)r^3\cos(3\theta+\alpha)\right]. \tag{35}$$

Proceeding to evaluate the second-order term w_2 from Eq. (7c) and noting that $L_1=\{w_1,\}$, we get

$$\frac{\partial w_2}{\partial s}=2K_2+2p_r[\kappa_2^{\mathrm{I}}(s)r\cos(2\theta)+\kappa_3^{\mathrm{I}}(s)r^2\cos(3\theta+\alpha)]-2l[\kappa_2^{\mathrm{I}}(s)\sin(2\theta)+\kappa_3^{\mathrm{I}}(s)r\sin(3\theta+\alpha)]. \tag{36}$$

Given that $\langle\kappa_2^{\mathrm{I}}\rangle=\langle\kappa_3^{\mathrm{I}}\rangle=0$, we must choose $K_2=0$ since there are no nonzero average terms. On integrating the above equation, we find

$$w_2=2p_r[\kappa_2^{\mathrm{II}}r\cos(2\theta)+\kappa_3^{\mathrm{II}}(s)r^2\cos(3\theta+\alpha)]-2l[\kappa_2^{\mathrm{II}}(s)\sin(2\theta)+\kappa_3^{\mathrm{II}}(s)r\sin(3\theta+\alpha)]. \tag{37}$$

Knowing w_2, we can proceed to the next order to calculate w_3 and K_3. Applying Eq. (7d) we get

$$\begin{aligned}\frac{\partial w_3}{\partial s}=&3K_3-3p_r^2[\kappa_2^{\mathrm{II}}(s)\cos(2\theta)+2\kappa_3^{\mathrm{II}}(s)r\cos(3\theta+\alpha)]+3lp_r[\kappa_3^{\mathrm{II}}(s)\sin(3\theta+\alpha)]\\&+3\frac{p_rl}{r}[2\kappa_2^{\mathrm{II}}(s)\sin(2\theta)+3\kappa_3^{\mathrm{II}}(s)r\sin(3\theta+\alpha)]+3\frac{l^2}{r^2}[2\kappa_2^{\mathrm{II}}(s)\cos(2\theta)+3\kappa_3^{\mathrm{II}}(s)r\cos(3\theta+\alpha)]\\&+[\kappa_2^{\mathrm{II}}(s)r\cos(2\theta)+\kappa_3^{\mathrm{II}}r^2\cos(3\theta+\alpha)][\kappa_2(s)r\cos(2\theta)+\kappa_3r^2\cos(3\theta+\alpha)]\\&+[\kappa_2^{\mathrm{II}}(s)\sin(2\theta)+\kappa_3^{\mathrm{II}}(s)r\sin(3\theta+\alpha)][\kappa_2(s)r^2\sin(2\theta)+\kappa_3(s)r^3\sin(3\theta+\alpha)]\end{aligned}$$

$$-\frac{1}{2}[\kappa_2^{\mathrm{I}}(s)r\cos(2\theta)+\kappa_3^{\mathrm{I}}(s)r^2\cos(3\theta+\alpha)]^2-\frac{1}{2}[\kappa_2^{\mathrm{I}}(s)r\sin(2\theta)+\kappa_3^{\mathrm{I}}(s)r^2\sin(3\theta+\alpha)]^2. \tag{38}$$

From Eqs. (31) and (32) one can easily identify the terms that average to zero over fast oscillations and those that do not. Once again K_3 is chosen such that it cancels the terms that average to a nonzero value. On simplifying certain averaged terms from integration by parts, the third-order transformed Hamiltonian may be expressed as

$$K_3=\tfrac{1}{2}\langle(\kappa_2^{\mathrm{I}})^2\rangle r^2-\tfrac{1}{3}\langle\kappa_2^{\mathrm{I}}\kappa_3^{\mathrm{I}}\rangle r^3\cos(\theta+\alpha)+\tfrac{1}{2}\langle(\kappa_3^{\mathrm{I}})^2\rangle r^4. \tag{39}$$

Since the Hamiltonian K is defined in the transformed coordinate system, the variables must be replaced by the corresponding transformed variables, R and Θ, in the above equation as well as in Eq. (34).

In order for K_3 to be independent of Θ, $\langle\kappa_2^{\mathrm{I}}\kappa_3^{\mathrm{I}}\rangle$ must vanish. It is clear from Eqs. (31) and (32) that one way this can be accomplished is if $\kappa_2(s)$ can be expressed as a pure cosine series and $\kappa_3(s)$ as a pure sine series. Figure 3 represents a practical design for $\kappa_2(s)$ and $\kappa_3(s)$ which satisfies this condition. This is a specific case where the two lattices have equal periodicity. In this case, $\kappa_2(s)$ and $\kappa_3(s)$ are periodic step functions alternating in sign and with opposite parity, which is equivalent to a phase lag of a quarter lattice period with respect to each other. It may be noted that once the Θ dependence is eliminated, the nonlinear force is purely focusing and leads to a positive tune shift. This design is only the simplest method of realizing optimum integrability and need not necessarily be the most practical one for real machines. However, the formulation of this condition is general enough to accommodate other designs that are possibly easier to implement. The general procedure to apply this is to first express $\kappa_2(s)$ and $\kappa_3(s)$ of an existing design in the form of Eqs. (31) and (32). Then the coefficient $\langle\kappa_2^{\mathrm{I}}\kappa_3^{\mathrm{I}}\rangle$ will need to be evaluated. This would then tell us how to reposition the magnets in order to minimize this. Numerical results in Sec. IV will show that considerable improvement in the dynamic aperture can be accomplished even if $\langle\kappa_2^{\mathrm{I}}\kappa_3^{\mathrm{I}}\rangle$ does not completely vanish but is small enough.

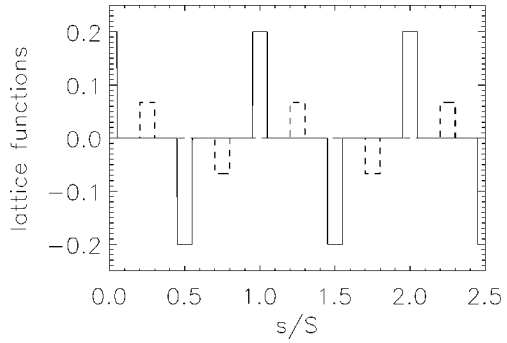

FIG. 3. A step function lattice that will lead to a near integrable condition. The shorter steps represent the sextupole function $\kappa_3(s)$ while the higher ones the quadrupole function $\kappa_2(s)$.

The purpose of choosing K_3 to be independent of Θ is to look for a system with improved integrability and thereby improve confinement by reducing chaos. According to the Kolmogorov-Arnold-Moser (KAM) theorem, a system perturbed from integrability will consist of regions of regular motion and regions of chaos with the latter approaching zero exponentially as the system approaches integrability. This system would be perfectly integrable if the Θ dependence could be completely eliminated. However, the fourth-order perturbation term will retain the Θ dependence. Despite this, the numerical results in the following sections will show that restricting the integrability up to third order makes a significant improvement in confinement in accordance with the KAM theorem. It is likely that a few mutipoles or other components such as undulators in synchrotron radiation sources cannot be incorporated in the averaging procedure. Another such example would be beam-beam interactions at interaction point of a storage ring collider where there might be many multipoles located at the same place. Superposing these additional effects randomly to the existing lattice would invariably make the system less integrable. In such a situation, it becomes even more important to obtain a system with optimum integrability since the KAM theorem would still guarantee that there exists a region in phase space with particles having regular trajectories. One could also consider using the method in Ref. [21] to implement the additional nonlinear components to a lattice that has already been designed to be nearly integrable using the method suggested here.

B. Alternate gradient quadrupoles, sextupoles, and octupoles

Although the analysis in the preceding section used only sextupoles, this can be extended to include higher multipoles. For example, if octupoles are used in addition to the sextupoles, the Hamiltonian would be

$$H=\frac{1}{2}\left(p_r^2+\frac{l^2}{r^2}\right)+\frac{1}{2}\kappa_2(s)r^2\cos(2\theta)+\frac{1}{3}\kappa_3(s)r^3\cos(3\theta+\alpha)+\frac{1}{4}\kappa_3(s)r^4\cos(4\theta+\gamma), \tag{40}$$

where γ represents the orientation of the octupoles. The third-order transformed Hamiltonian will then be

$$K_3=\tfrac{1}{2}\langle(\kappa_2^{\mathrm{I}})^2\rangle r^2+\tfrac{1}{2}\langle(\kappa_3^{\mathrm{I}})^2\rangle r^4+\tfrac{1}{2}\langle(\kappa_4^{\mathrm{I}})^2\rangle r^6-\tfrac{1}{3}\langle\kappa_2^{\mathrm{I}}\kappa_3^{\mathrm{I}}\rangle r^3\cos(\theta+\alpha)-\tfrac{1}{3}\langle\kappa_2^{\mathrm{I}}\kappa_4^{\mathrm{I}}\rangle r^4\cos(2\theta+\gamma)-\tfrac{1}{3}\langle\kappa_3^{\mathrm{I}}\kappa_4^{\mathrm{I}}\rangle r^5\cos(\theta+\alpha+\gamma). \tag{41}$$

The conditions $\langle\kappa_2^{\mathrm{I}}\kappa_3^{\mathrm{I}}\rangle=0$, $\langle\kappa_2^{\mathrm{I}}\kappa_4^{\mathrm{I}}\rangle=0$, and $\langle\kappa_3^{\mathrm{I}}\kappa_4^{\mathrm{I}}\rangle=0$ would

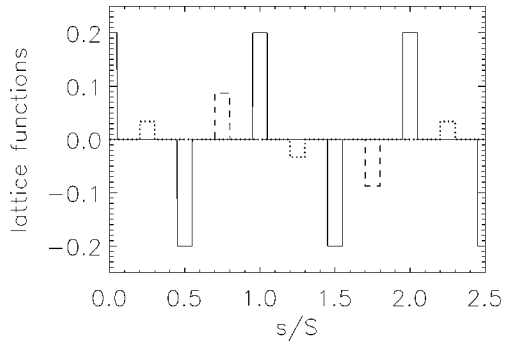

FIG. 4. A step function lattice leading to a near integrable condition. The shortest steps represent the octupole function $\kappa_4(s)$, while the higher ones the sextupole function $\kappa_3(s)$, and the highest ones the quadrupole function $\kappa_2(s)$.

optimize the integrability of such a system. A practical but idealized design for this to be satisfied is given in Fig. 4.

V. SINGLE-PARTICLE TRAJECTORIES WITH NONZERO ANGULAR MOMENTUM

To show that particles are better confined when the 90° phase difference condition is satisfied, numerical calculations were performed using the original Hamiltonian. The results are discussed in this and the following sections. Calculations were performed using a fourth-order symplectic integrator [19,20] in Cartesian coordinates. Cartesian coordinates are more convenient for numerical calculations as they enable one to avoid the singularity at the origin arising in the cylindrical coordinate system. The focusing channel consisted of alternating gradient quadrupoles and sextupoles with various phase differences between $\kappa_2(s)$ and $\kappa_3(s)$. The sextupoles were oriented such that $\alpha=-45°$. In Cartesian coordinates, the force due to quadrupoles is given by

$$\vec{F} = \kappa_2(s)(x\hat{x} - y\hat{y}). \tag{42}$$

and that due to the sextupoles (with $\alpha=-45°$) is given by

$$\vec{F} = \kappa_3(s)[(x^2 - y^2 + 2xy)\hat{x} + (x^2 - y^2 - 2xy)\hat{y}]. \tag{43}$$

We define a radial distance $R=\frac{1}{3}|\kappa_2|/|\kappa_3|$, where $|--|$ corresponds to the positive nonzero values of the respective step function. The ratio $|\kappa_2|/|\kappa_3|$ represents a measure of the position where the forces due to the linear and nonlinear components become comparable. The tune shift due to the nonlinear force was close to 15% for a particle initially at $r=R$ and $\theta=45°$. The fill factor η is defined as the ratio between the length of the magnets and the length of one lattice period. This was set to 0.2 for both, the quadrupoles and sextupoles. This is typical for most applications. For example, the storage ring of the advanced photon source has a fill factor of about 0.21 for quadrupoles. When expressed in units of S, η is the smallest time scale to be resolved and so the time step in the computation needs to be much smaller than η. In all the computations, this time step was set to 0.01η. The parameter $\kappa_2(s)$ has units of frequency squared so we can define another dimensionless quantity as $|\kappa_2|S^2$ to which the value of 8.0 was assigned for all calculations. This corresponds to about seven lattice periods per betatron radial oscillation about the origin. The separation between the quadrupoles and sextupoles is represented by a term

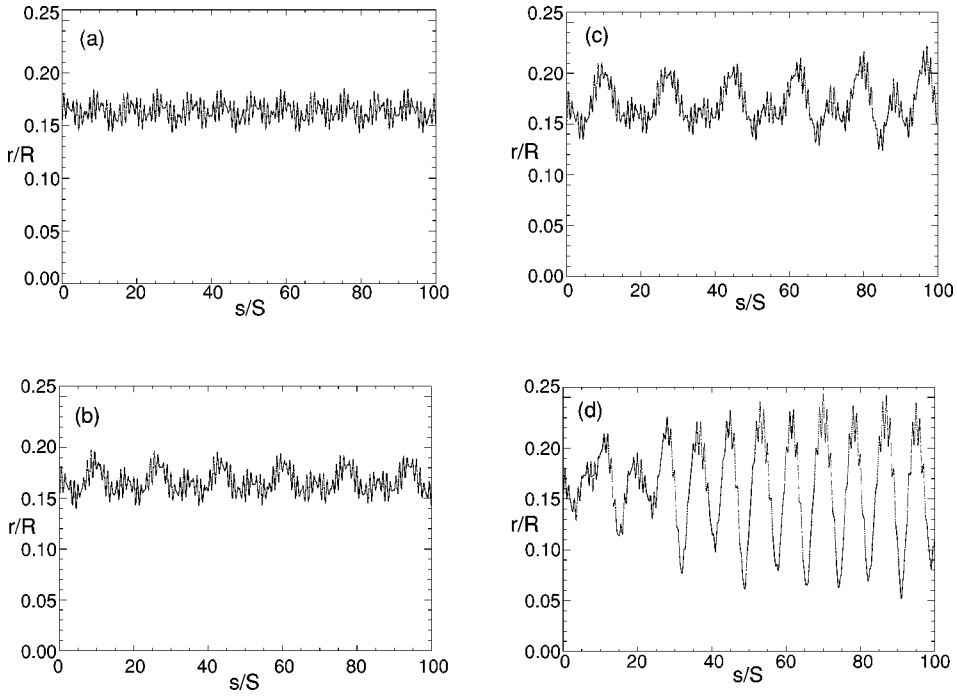

FIG. 5. Radial oscillation of particles for (a) $\psi=90°$, (b) $\psi=60°$, (c) $\psi=30°$, (d) $\psi=0°$.

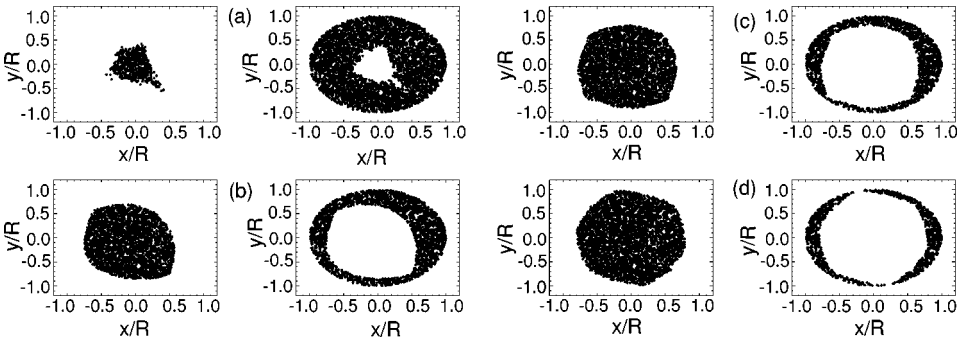

FIG. 6. Initial distribution of confined and unconfined particles lying on the x-y plane for ψ= (a) 0°, (b) 30°, (c) 60°, (d) 90°.

$$\psi = \frac{2\pi\Delta s}{S}, \tag{44}$$

where Δs is the spatial distance between the two of them. The averaged Hamiltonian K is independent of Θ when $\psi = 90°$, i.e., when the sextupoles are placed halfway between two quadrupoles of opposite sign. The values of R, η, $|\kappa_2|S^2$, and ψ completely specify the focusing system.

When a system is azimuthally symmetric, angular momentum is conserved. In this system, when $\psi = 90°$, the angular momentum is nearly conserved because the averaged angular momentum is azimuthally symmetric. As one deviates from $\psi = 90°$, the dependence on θ becomes stronger and the variation of angular momentum becomes more significant. This would lead to increased chaotic motion. In order to verify this, as an example, we examined the trajectory of a particle at $r = 0.15R$. The particle had an initial velocity of $0.05R/S$ in a direction perpendicular to its initial displacement.

The results of these calculations with respect to different values of ψ are shown in Fig. 5. The rapid variation in amplitude represents the lattice oscillations. The values of ψ used were 90°, 60°, 30°, and 0°, respectively. It is clear that there is a transition to chaotic motion as ψ deviates from 90°. For $\psi = 90°$, the maximum amplitude of oscillation is relatively small. When ψ changes to 60°, the maximum amplitude increases. At $\psi = 60°$, we see that additional frequency components are added to the oscillation. When $\psi = 0$, the sextupoles and quadrupoles overlap. In this situation the motion is chaotic. There is no observable repetition in the motion of the particle and it travels well beyond the maximum radial distance attained in the $\psi = 90°$ case. This transition would have been more rapid if the initial position of the particle was further away from the center. It is sufficient to examine cases where the phase lag between the quadrupoles and sextupoles, ψ, varies from 0° to 90°. Phase differences outside this range can be mapped back to a corresponding point between 0° and 90° by making an appropriate linear transformation in θ.

The requirement of reduced chaos becomes important when sextupoles or other higher multipoles are present in certain segments of a storage ring where this segment is periodically encountered by the particles. With reduced integrability, the motion becomes sensitive to the initial conditions of the particle at the entrance of the segment. This would eventually lead to increase in oscillation amplitude in the rest of the channel and consequently limit the dynamic aperture of the storage ring.

VI. ESTIMATION OF DYNAMIC APERTURE FOR DIFFERENT CASES

The dynamic aperture is defined as the volume in phase space in which all particles remain confined throughout their trajectories in the accelerator. The calculations in this section estimate the projection of the dynamic aperture onto various phase space planes for different values of ψ. In order to perform these calculations, we used 5000 particles that were initially distributed uniformly over the respective plane in phase space, and these were then evolved for 500 lattice periods. It was assumed that particles that travel beyond $r = R$ at any time during this period are not confined. After

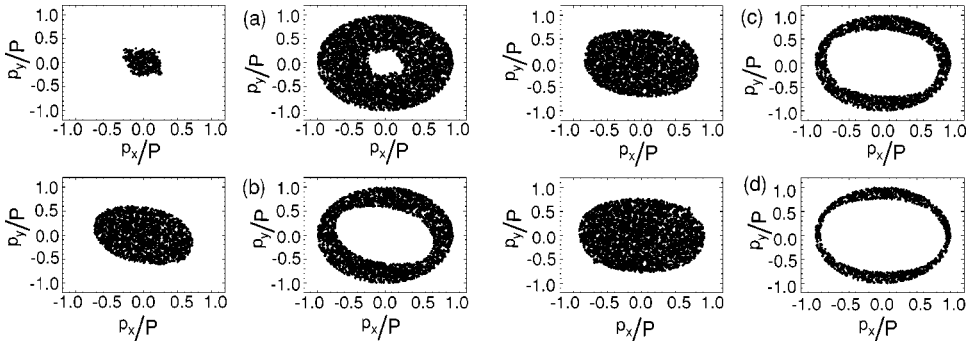

FIG. 7. Initial distribution of confined and unconfined particles lying on the p_x-p_y plane for ψ= (a) 0°, (b) 30°, (c) 60°, (d) 90°.

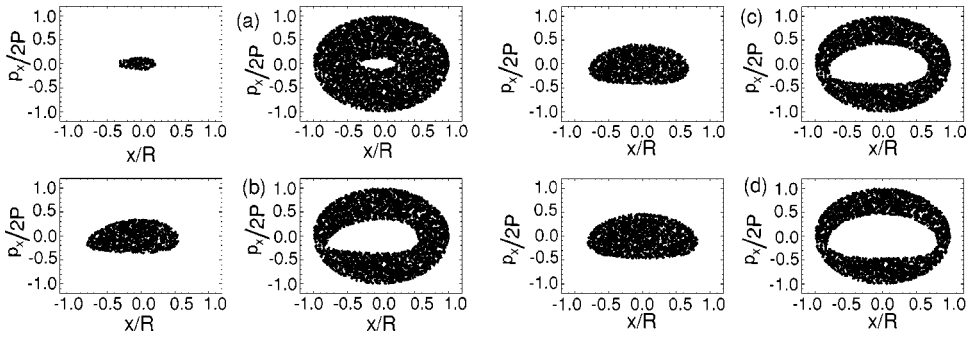

FIG. 8. Initial distribution of confined and unconfined particles lying on the x-p_x plane for ψ= (a) 0°, (b) 30°, (c) 60°, (d) 90°.

identifying the particles that remain confined and those that do not, the initial distribution was separated and the positions of these two sets of particles were plotted. In Figs. 6–8 the left side represents the initial phase space positions of confined particles and the ones on the right represent the unconfined particles from the same initial distribution. It is important to plot the confined and unconfined particles separately in order to ensure that there is no overlap between the two regions, which is true in these simulations. This is expected because all the phase space variables other than those shown in the respective plot were set to zero. Given that the dynamic aperture allows only confined particles and not a mixture of the two, the left side plots represent the projection of the dynamic aperture onto the respective plane.

Figure 6 shows particles lying in the x-y plane that were all initially at rest and distributed uniformly within a circle of radius $r=R$. It may be noticed that when ψ is 0°, a very small number of these particles are confined. This is the case when the quadrupoles and sextupoles completely overlap. The confinement increases very rapidly as one deviates from $\psi=0°$. The area containing the confined particles then gradually increases, reaching a maximum when $\psi=90°$ as predicted by the analytic result of the preceding section. Another interesting feature revealed by these plots is that the area of confinement acquires sharper corners with increasing ψ.

Figure 7 shows confined and unconfined particles from the initial distribution spread out in momentum space. These particles are all located initially at $x=y=0$ and distributed uniformly within a circle of radius $P=0.44R/S$. Once again, a rapid improvement in confinement is seen as one deviates from $\psi=0°$ and there is then a gradual improvement as ψ approaches 90°. Unlike the previous case, the boundary of the region of confinement is smooth for all values of ψ. We also see that the dynamic aperture attains a more circular shape for $\psi=90°$ which could be attributed to weaker dependence of the dynamics on θ.

Figure 8 shows particles distributed over an ellipse such that

$$\frac{x^2}{R^2}+\frac{p_x^2}{(2P)^2}<1, \tag{45}$$

while all other phase space values are zero. Qualitatively, the same behavior is noticeable as in the previous cases. The figures also show that the shape of the dynamic aperture exhibits less symmetry about the origin along the x axis as ψ decreases from 90°. This is also a reflection of increased symmetry in the dynamics along θ.

In contrast to the dramatic improvement in the dynamic aperture seen when ϕ was close to zero, there was only a small improvement when ψ changed from 60° to 90°. This phenomena is important in applications where it is not possible to achieve the idealized condition due to other practical limitations often demanding that such theoretically derived conditions be sufficiently robust to be useful. Improvement in the region of confinement, which is directly related to increased size of the dynamic aperture is an important aspect in improving the performance of particle accelerators. It has been shown how the presence of higher order poles can limit the size of the dynamic aperture in circular accelerators [22].

VII. SUMMARY

In this paper, a condition for improved dynamic aperture is derived for nonlinear lattices in particle accelerators. To start with, the Lie transform perturbation method is presented for averaging over fast time scales. The validity of the method is first verified numerically for a linear periodic focusing system. This averaging procedure is then applied to nonlinear focusing systems with quadrupoles and sextupoles. The Hamiltonian of this system contains terms with mixed variables, a situation in which the Lie transform method greatly simplifies the analysis. This analysis yields a condition for the Hamiltonian to have increased symmetry thereby reducing chaos and increasing the dynamic aperture. The condition leads to a canonical transformation where the new Hamiltonian is independent of its azimuthal variable up to third order in the perturbation expansion. While the analysis was performed explicitly for a lattice with quadrupoles and sextupoles, it was straightforward to show that similar conditions exist when even higher order mutipoles or combinations of these are used. Unlike the traditional approach of analyzing a nonlinear lattice, no assumption was made that the nonlinear focusing was small compared to the linear focusing strength. Hence this analysis is valid even when the nonlinearity is strong enough that the closed form Courant-Snyder solutions are not valid.

Numerical calculations were performed for a particular case in which the focusing components were quadrupoles and sextupoles represented by periodic step function lattices

of equal periodicity. In this case, the condition of azimuthal symmetry in the transformed frame was satisfied by having a phase difference of $\psi=90°$, equivalent to a quarter of a lattice period between the quadrupoles and sextupoles. Single-particle trajectories of particles with angular momentum showed increased chaotic behavior as ψ decreased from 90° to 0°. The size of the dynamic aperture was estimated by allowing the particles to drift up to a maximum radial distance which allowed a maximum tune shift of about 15% when compared to arbitrarily small oscillations. Calculations showed that the size of the dynamic aperture increased rapidly as ψ increased from 0° and gradually reached a maximum as ψ approached 90°. Results showed that the condition was robust enough for possible practical applications.

While the parameters used in the calculations were realistic, they were also simplified. This theory remains to be applied to parameters specific to real machines. For example, it would be interesting to apply it in the use of sextupoles for chromaticity corrections in storage rings with their lattice periods different from that of the quadrupoles and also having a different fill factor. This would still allow conditions for a near integrable system and so one should expect improved confinement by imposing the same.

The derivation of the symmetric transformed Hamiltonian in this paper is expected to benefit various current and proposed applications of nonlinear lattices in particle accelerators. It would also add to previous work on increasing the dynamic aperture of accelerator lattices in the presence of nonlinear components [21]. The Lie transform perturbation method presented here is easily applicable to other areas of Hamiltonian dynamics as well where it is required to perform a time averaging over certain fast time scales.

ACKNOWLEDGMENTS

One of us (K.S.G.) wishes to acknowledge Jim Howard for many useful suggestions. This work was supported by the U.S. Department of Energy under Grant No. DE-FG03-95ER40926.

[1] E. D. Courant and H. S. Snyder, Ann. Phys. (N.Y.) **3**, 1 (1958).
[2] N. Tsoupas, M. Zucker, T. Ward, and C. Snead, Nucl. Sci. Eng. **126**, 71 (1997).
[3] Y. K. Batygin, Phys. Rev. E **57**, 6029 (1998).
[4] Y. K. Batygin, Phys. Rev. E **53**, 5358 (1996).
[5] C. Montag, J. Kewisch, D. Trbojevic, and F. Schmidt, Phys. Rev. ST Accel. Beams **5**, 084401 (2002).
[6] L. Tosi, V. Samaluk, and E. Karantzoulis, Phys. Rev. ST Accel. Beams **6**, 054401 (2003).
[7] L. F. Wang, H. Fukuma, S. Kurokawa, and K. Oide, Phys. Rev. E **66**, 036502 (2002).
[8] J. Gao, Nucl. Instrum. Methods Phys. Res. A **463**, 50 (2001).
[9] P. Channel, Phys. Plasmas **6**, 982 (1999).
[10] R. C. Davidson and H. Qin, Phys. Rev. ST Accel. Beams **4**, 104401 (2001).
[11] S. Tzenov and R. C. Davidson, Phys. Rev. ST Accel. Beams **5**, 021001 (2002).
[12] J. R. Cary, Phys. Rep. **79**, 129 (1981).
[13] G. Hori, Publ. Astron. Soc. Jpn. **18**, 287 (1966).
[14] L. M. Garrido, J. Math. Phys. **10**, 1045 (1968).
[15] A. Deprit, Celest. Mech. **1**, 12 (1969).
[16] R. L. Dewar, J. Phys. A **9**, 2043 (1976).
[17] A. J. Dragt and J. M. Finn, J. Math. Phys. **17**, 2215 (1976).
[18] A. Lichtenberg and M. Lieberman, *Regular and Chaotic Dynamics* (Springer-Verlag, Berlin, 1992).
[19] E. Forest and R. Ruth, Physica D **43**, 105 (1990).
[20] J. Candy and W. Rozmus, J. Comp. Physiol. **92**, 230 (1991).
[21] W. Wan and J. R. Cary, Phys. Rev. Lett. **81**, 3655 (1998).
[22] J. Gao, Nucl. Instrum. Methods Phys. Res. A **451**, 545 (2000).